Low-threshold-current-density 1300-nm dilute-nitride quantum well lasers

Nelson Tansu,[a)] Nicholas J. Kirsch, and Luke J. Mawst

Reed Center for Photonics, Department of Electrical Computer Engineering, University of Wisconsin-Madison, 1415 Engineering Drive, Madison, Wisconsin 53706-1691

Metalorganic chemical vapor deposition-grown $In_{0.4}Ga_{0.6}As_{0.995}N_{0.005}$ quantum well (QW) lasers have been realized, at an emission wavelength of 1.295 μm, with threshold and transparency current densities as low as 211 A/cm^2 (for $L=2000$ μm) and 75 A/cm^2, respectively. The utilization of a tensile-strained $GaAs_{0.67}P_{0.33}$ buffer layer and $GaAs_{0.85}P_{0.15}$ barrier layers allows a highly-compressively-strained $In_{0.4}Ga_{0.6}As_{0.995}N_{0.005}$ QW to be grown on a high-Al-content lower cladding layer, resulting in devices with high current injection efficiency ($\eta_{inj} \sim 97\%$). © *2002 American Institute of Physics.* [DOI: 10.1063/1.1511290]

The dilute-nitride quantum well (QW) on GaAs substrate, to achieve 1300-nm wavelength emission, has been a very promising choice active region in realizing high-performance long-wavelength GaAs-based vertical cavity surface emitting lasers (VCSELs).[1–12] Less temperature sensitivity in InGaAsN QW lasers, at $\lambda=1300$ nm, has also been demonstrated in many of the published results.[1–12] Although the area of temperature sensitivity in InGaAsN QW lasers is still under extensive investigation,[13,14] promising results of both low threshold-current-density (J_{th}) and high T_0 values $[1/T_0=(1/J_{th})dJ_{th}/dT]$ have been demonstrated.[3,6,12] Recently, efforts to achieve high performance InGaAsN QW lasers by metalorganic chemical vapor deposition (MOCVD)[3–7] have been pursued. The advantage of the MOCVD-grown InGaAsN QW lasers is the ease in growing high quality AlAs/GaAs distributed Bragg reflectors by MOCVD, compared to molecular beam epitaxy (MBE) techniques, for realizing low-cost VCSELs. Only recently, MOCVD-grown InGaAsN QW lasers,[3–7] at $\lambda=1300$ nm, have demonstrated comparable performances with the MBE-grown InGaAsN QW lasers.[8–12]

As shown in our earlier studies,[3] tensile-strained buffer layers (InGaP+GaAsP) are crucial for achieving highly strained InGaAs(N) QW lasers grown on thick, high-Al-content (75%–85%) AlGaAs lower cladding layers. In the present work, we report very low threshold (J_{th})- and transparency (J_{th})-current-density, strain-compensated $In_{0.4}Ga_{0.6}As_{0.995}N_{0.005}$ QW lasers with high current injection efficiency (η_{inj}) by utilizing strain compensation from GaAsP tensile-strained barriers and a thin GaAsP tensile-strained buffer layer.

The lasers structures utilized here were all grown by low-pressure MOCVD. Trimethylgallium, trimethylaluminium, and trimethylindium are used as the group III sources and AsH$_3$, PH$_3$, and U-dimethylhydrazine (U-DMHy) are used as the group V sources. The dopant sources are SiH$_4$ and dielthylzinc for the *n*- and *p*-dopants, respectively. The laser structure, shown in Fig. 1, utilizes a 60-Å highly compressively-strained ($\Delta a/a=2.7\%$) $In_{0.4}Ga_{0.6}As_{0.995}N_{0.005}$ QW, as the active region. The typical

peak photoluminescence wavelength of the 60-Å $In_{0.4}Ga_{0.6}As_{0.995}N_{0.005}$ QW is approximately 1290–1310 nm, with variations in emission wavelength resulted from run-to-run variations and nonuniformity across the wafer. The lower- and top-cladding layers of the lasers consist of $Al_{0.74}Ga_{0.26}As$ layers with doping levels of 1×10^{18} cm^3 for both the *n*- and *p*-cladding layers, respectively. The growth temperatures of the *n*- and *p*-$Al_{0.74}Ga_{0.26}As$ are 775 and 640 °C, respectively. The annealing of the InGaAsN QW is accomplished during the growth of the top cladding layer at temperature of 640 °C, with duration of approximately 27 min. This annealing condition does not represent the optimized annealing temperature and duration for the InGaAsN QW, yet this condition is sufficient for achieving strong luminescence from the QW. The InGaAsN QW is surrounded by tensile-strain barriers of $GaAs_{0.85}P_{0.15}$ ($\Delta a/a=0.6\%$), which are spaced 100 Å on each side of the QW. Earlier studies have demonstrated that the utilization of the GaAsP tensile-strained barriers surrounding the highly-compressively-strained InGaAsN QW results in improved optical luminescence.[3] The tensile buffer for this structure consists of a 30-Å $GaAs_{0.67}P_{0.33}$ layer, which eliminates the poor interface of the InGaP–GaAs in our earlier structures.[3]

One of the challenges in growing InGaAsN QW lasers by MOCVD is due to the difficulties in incorporating N into the InGaAs QW, while maintaining a high optical quality film. The low purity of the N precursor used in MOCVD (U-DMHy) is also suspected as a possible reason for the low optical quality of MOCVD-grown InGaAsN QWs. In order
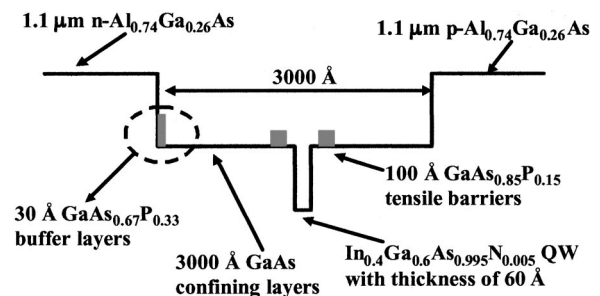

FIG. 1. Schematic energy bandgap diagram for the $In_{0.4}Ga_{0.6}As_{0.995}N_{0.005}$–$GaAs_{0.85}P_{0.15}$ QW laser structure with tensile buffer layer of 30-Å $GaAs_{0.67}P_{0.33}$.

[a)]Electronic mail: tansu@cae.wisc.edu

TABLE I. Performance and extracted intrinsic device parameters of $In_{0.4}Ga_{0.6}As_{0.995}N_{0.005}$ QW diode lasers with 100-μm-stripe-width devices, and comparison with the published results on InGaAsN QW lasers.

	Growth	L (μm)	J_{th} (A/cm^2)	J_{tr} (A/cm^2)	η_d (%)	η_{inj} (%)	α_i (cm^{-1})	λ (μm)	T_0 (K)	T_1 (K)
Livshits et al.[a]	MBE	3200	270	110	45	93	4	1.3	75	⋯
		1000	405	110	70	93	4	1.3	75	⋯
Ha et al.[b]	MBE	770	1500	⋯	47			1.315	65	
Peng et al.[c]	MBE	1600	546	227	50	80	7	1.317	104	⋯
Wei et al.[d]	GS-MBE	3000	1150	⋯	23	82	9.76	1.3	122	⋯
Hohnsdorf et al.[e]	MOCVD	800	800		37	75	15	1.28	60	⋯
Sato et al.[f]	MOCVD	960	920	⋯	⋯	⋯	⋯	1.29	150	⋯
Kawaguchi et al.[g]	MOCVD	1250	450	⋯	⋯	⋯	⋯	1.28	205	⋯
Takeuchi et al.[h]	MOCVD	1000	580	⋯	⋯	⋯	⋯	1.29	⋯	⋯
Tansu et al.[i]	MOCVD	750	400	110	51	72	6	1.29	110	416
		1500	289	110	40	72	6	1.295	130	400
Present Work	MOCVD	720	361	75	57	97	13	1.29	82	360
		1000	253	75	46	97	13	1.294	88	255
		2000	211	75	33	97	13	1.295	90	200

[a]See Ref. 8
[b]See Ref. 11
[c]See Ref. 12
[d]See Ref. 9
[e]See Ref. 7
[f]See Ref. 5
[g]See Ref. 6
[h]See Ref. 4
[i]See Ref. 3

to incorporate sufficient N into the InGaAsN QW, very large [DMHy]/V (as high as 0.961) is required. Due to the high cost and the low purity of the DMHy precursor, lowering the [AsH$_3$]/III to achieve large [DMHy]/V would be the preferable option to increasing the DMHy flow. Large [DMHy]/V ratio requires the [AsH$_3$]/III ratio to be rather low. Takeuchi et al.[15] have demonstrated that the growth of InGaAs QW (λ=1200 nm) with the *very low* [AsH$_3$]/III ratio is significantly more challenging compared to the case in which tertiary butyl arsine (TBA) is utilized as the As precursor. As the [AsH$_3$]/III ratio is reduced, the luminescence of the InGaAs QW reduces rapidly for low [AsH$_3$]/III (below 15–20), which is, however, required for achieving sufficiently large [DMHy]/V. These challenges have resulted in difficulties in realizing high performance MOCVD-InGaAsN QW lasers with AsH$_3$ as the As precursor until recently.[3,4,6,7] In our approach, the design of the active region is based on strain-compensated InGaAsN QW, with very high In content (In~40%) and minimum N content (N~0.5%), to achieve 1300-nm emission. Minimum N content in the InGaAsN QW allows us to grow the active region with an optimized AsH$_3$/III ratio.

In characterizing our laser performance of the InGaAsN QW lasers, broad area lasers with stripe width of 100 μm are fabricated. The conventional multilength studies of various broad area devices, with cavity length (L) ranging from 720 μm to 3000 μm, are utilized to extract the intrinsic device parameters. All the measurements of these broad area devices were performed under pulsed conditions with pulsed width of 6 μs, and 1% duty cycle. All the measured parameters and extracted intrinsic device parameters for these lasers are summarized in Table I, under the section "Present Work."

The measured threshold current density, at room temperature of 20 °C, for the InGaAsN QW lasers, is shown in Fig. 2 for various cavity length devices. The threshold- and transparency-current density are measured to be as low as 211 and 75 A/cm^2, respectively, for devices with cavity length of 2000 μm, and emission wavelength of 1.295 μm. Even for shorter cavity devices of 720 μm and 1000 μm, threshold-current densities are measured to be as low as 361 and 253 A/cm^2, respectively. To the best of our knowledge, these data represent the lowest threshold- and transparency-current densities reported for InGaAsN QW lasers in the wavelength regime of 1.28–1.32 μm as shown in Table I.[1–12]

The external differential quantum efficiency (η_d) of the InGaAsN QW lasers, as shown in Fig. 3, is as high as 57% for devices with cavity lengths of 720 μm. The lower η_d for the longer cavity devices is attributed to the relatively large internal loss (α_i=13 cm^1) for these unoptimized structures. The internal loss of the lasers may result from the combination of the narrow separate-confinement-heterostructure (SCH) region and relatively high doping level ($1-2 \times 10^{18}$ cm^{-3}) of the p-cladding of the laser.

Reduction in the current injection efficiency in QW lasers can result from large recombination in the SCH and also nonradiative processes in the interface between the SCH-cladding layers. The poor interface between the InGaP buffer layer and GaAs SCH region in our previous structure is believed to have been responsible for the low current injection
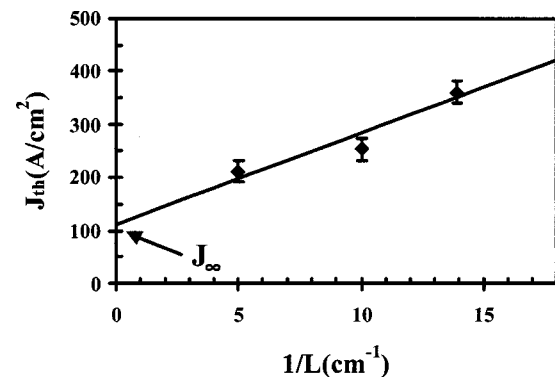

FIG. 2. The room-temperature threshold current density (J_{th}) of the $In_{0.4}Ga_{0.6}As_{0.995}N_{0.005}$–$GaAs_{0.85}P_{0.15}$ QW as a function of inverse cavity length (1/L).
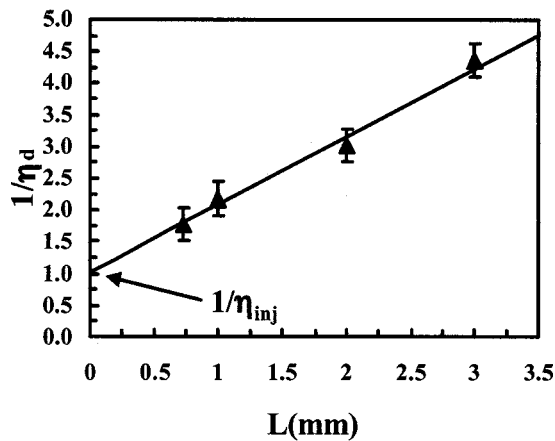
FIG. 3. The room-temperature inverse of the η_d of the $In_{0.4}Ga_{0.6}As_{0.995}N_{0.005}-GaAs_{0.85}P_{0.15}$ QW as a function of cavity length (L).

efficiencies ($\eta_{inj}=72\%$) observed,[3] resulting from nonradiative recombination in the interface. By utilizing a thin GaAsP buffer layer in place of InGaP+GaAsP buffer layer,[3] improvement in the current injection efficiencies ($\eta_{inj}=97\%$) has been achieved as a result of the removal of the poor interface of InGaP buffer and GaAs SCH.

The material gain parameter, defined as $g_{oJ}=g_{th}/\ln(\eta_{inj}\cdot J_{th}/J_{tr})$, is an important parameter in determining the gain properties of the QW. A low g_{oJ} value for a QW laser can result from the low optical gain of material $[g_{oN}=g_{th}/\ln(n_{th}/n_{tr})]$ or the existence of nonradiative recombination in QW. The material-gain parameter (g_{oJ})[3] and the differential gain (dg/dn)[16] of the InGaAsN QW have been shown to decrease as nitrogen is introduced into the InGaAs QW. As shown in Fig. 4, the g_{oJ} of the InGaAsN QW laser is measured to be 1150 cm^{-1}, which is significantly lower that ($g_{oJ}=1600-1900$ cm^{-1}) of similar InGaAs QW lasers[2,3] at $\lambda=1.17-1.19$ μm.

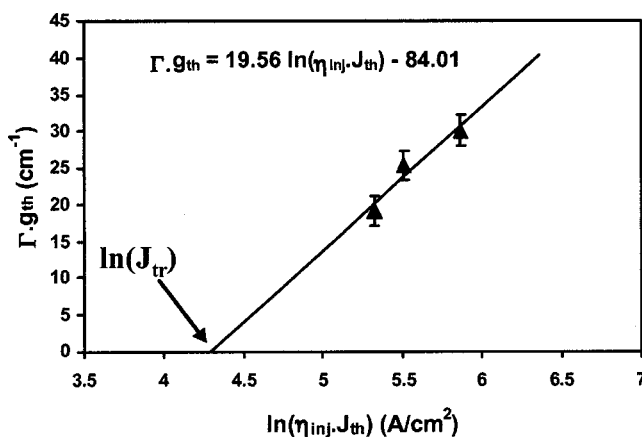FIG. 4. Semilogarithmic linear regression of the modal gain ($\Gamma \cdot g$) of the $In_{0.4}Ga_{0.6}As_{0.995}N_{0.005}$ QW as a function of logarithmic of the internal current density ($\eta_{inj} \cdot J$).

The $In_{0.4}Ga_{0.6}As_{0.995}N_{0.005}$ QW lasers, with emission wavelength of 1.29–1.295 μm, exhibit relatively low temperature sensitivity, with T_0 values of 82–90 K for devices with cavity length of 720–2000 μm at a temperature range of 20–60 °C. The T_1 values $[1/T_1=-(1/\eta_d)(d\eta_d/dt)]$ are measured from 200 to 360 K, for devices with L of 720–2000 μm. The expected length dependence of T_0 and T_1 is due to the variation of threshold gain with cavity length.[13] In analyzing these T_0 values, one has to consider the fact that high-J_{th} QW lasers with large monomolecular recombination will result in devices with high T_0 values.[13] Relatively low T_0 values for low-J_{th} InGaAsN QW lasers can result from carrier leakage,[13] temperature-sensitive gain,[13] and/or Auger recombination.[14]

In summary, high-performance strain-compensated $In_{0.4}Ga_{0.6}As_{0.995}N_{0.005}$ QW lasers, with a lasing emission wavelength of 1.295 μm, have been achieved by MOCVD utilizing AsH$_3$ as the As precursor. Threshold (J_{th})- and transparency (J_{tr})-current densities of the InGaAsN QW lasers have been measured to be 211 A/cm^2 ($L=2000$ μm) and 75 A/cm^2, respectively. The utilization of a thin GaAsP tensile-strained buffer layer results in devices with high η_{inj} of 97%. To the best of our knowledge,[1–12] these threshold- and transparency-current densities (as shown in Table I) are the lowest values reported to date for 1280–1320 nm InGaAsN QW lasers.

[1] M. Kondow, T. Kitatani, S. Nakatsuka, M. C. Larson, K. Nakahara, Y. Yazawa, M. Okai, and K. Uomi, IEEE J. Sel. Top. Quantum Electron. **3**, 719 (1997).

[2] N. Tansu and L. J. Mawst, IEEE Photonics Technol. Lett. **13**, 179 (2001).

[3] N. Tansu and L. J. Mawst, IEEE Photonics Technol. Lett. **14**, 444 (2002).

[4] T. Takeuchi, Y.-L. Chang, M. Leary, A. Tandon, H.-C. Luan, D. P. Bour, S. W. Corzine, R. Twist, and M. R. Tan, IEEE LEOS 2001 Post-Deadline Session 2001).

[5] S. Sato, Jpn. J. Appl. Phys. **39**, 3403 (2000).

[6] M. Kawaguchi, T. Miyamoto, E. Gouardes, D. Schlenker, T. Kondo, F. Koyama, and K. Iga, Jpn. J. Appl. Phys. **40**, L744 (2001).

[7] F. Hohnsdorf, J. Koch, S. Leu, W. Stolz, B. Borchert, and M. Druminski, Electron. Lett. **35**, 571 (1999).

[8] D. A. Livshits, A. Yu. Egorov, and H. Riechert, Electron. Lett. **36**, 1381 (2000).

[9] J. Wei, F. Xia, C. Li, and S. R. Forrest, IEEE Photonics Technol. Lett. **14**, 597 (2002).

[10] K. D. Choquette, J. F. Klem, A. J. Fischer, O. Blum, A. A. Allerman, I. J. Fritz, S. R. Kurtz, W. G. Breiland, R. Sieg, K. M. Geib, J. W. Scott, and R. L. Naone, Electron. Lett. **36**, 1388 (2000).

[11] W. Ha, V. Gambin, M. Wistey, S. Bank, S. Kim, J. S. Harris, Jr., IEEE Photonics Technol. Lett. **14**, 591 (2002).

[12] C. S. Peng, T. Jouhti, P. Laukkanen, E.-M. Pavelescu, J. Konttinen, W. Li, and M. Pessa, IEEE Photonics Technol. Lett. **14**, 275 (2002).

[13] N. Tansu and L. J. Mawst, IEEE Photonics Technol. Lett. **14**, 1052 (2002).

[14] R. Fehse, S. J. Sweeney, A. R. Adams, E. P. O'Reilly, A. Y. Egorov, H. Riechert, and S. Illek, Electron. Lett. **37**, 92 (2000).

[15] T. Takeuchi, Y.-L. Chang, A. Tandon, D. Bour, S. Corzine, R. Twist, M. Tan, and H.-C. Luan, Appl. Phys. Lett. **80**, 2445 (2002).

[16] S. Tomic and E. P. O'Reilly (in press).